

Journal of Materials Chemistry C

Accepted Manuscript



This article can be cited before page numbers have been issued, to do this please use: S. Liu, H. Yu, Q. Zhang, F. Qin, X. Zhang, L. Zhang and W. Xie, *J. Mater. Chem. C*, 2019, DOI: 10.1039/C9TC00648F.



This is an Accepted Manuscript, which has been through the Royal Society of Chemistry peer review process and has been accepted for publication.

Accepted Manuscripts are published online shortly after acceptance, before technical editing, formatting and proof reading. Using this free service, authors can make their results available to the community, in citable form, before we publish the edited article. We will replace this Accepted Manuscript with the edited and formatted Advance Article as soon as it is available.

You can find more information about Accepted Manuscripts in the [author guidelines](#).

Please note that technical editing may introduce minor changes to the text and/or graphics, which may alter content. The journal's standard [Terms & Conditions](#) and the ethical guidelines, outlined in our [author and reviewer resource centre](#), still apply. In no event shall the Royal Society of Chemistry be held responsible for any errors or omissions in this Accepted Manuscript or any consequences arising from the use of any information it contains.

ARTICLE

Efficient ITO-free organic light-emitting devices with dual-functional PSS-rich PEDOT:PSS electrode by enhancing carrier balance

Cite this: DOI: xxxxxx

Received xxxx,
Accepted xxxx

DOI: xxxxxx

www.rsc.org/

Shihao Liu, Hongwei Yu, Qingyang Zhang, Feisong Qin, Xiang Zhang, Letian Zhang*, Wenfa Xie*

State Key Laboratory of Integrated Optoelectronics, College of Electronic Science and Engineering, Jilin University, Changchun, 130012, People's Republic of China. *E-mail: zlt@jlu.edu.cn, xiewf@jlu.edu.cn

Organic semiconductors typically show highly asymmetric hole and electron mobilities, with the hole mobility exceeding the electron mobility by orders of magnitude in most cases. Therefore, extra hole buffer layer is always needed to alleviate the hole injection, complicating the fabrication of organic light-emitting devices (OLEDs). Here, bifunctional electrode serving as transparent electrode and hole buffer layer simultaneously is proposed by using highly conductive poly(3,4-ethylenedioxythiophene) polystyrene sulfonate (PEDOT:PSS) films without removing any PSS chains. The existence of a large number of PSS chains makes these PEDOT:PSS electrode possible to possess hole buffer functions. Much better carrier balance can be achieved in the OLEDs based on the dual-functional electrode. Till now, although it's still a challenge to achieve high performance OLEDs based on PEDOT:PSS transparent electrode, this type of OLEDs, including green and white devices, show excellent luminous efficiency and efficiency roll-off, much better than ITO-based devices. It provides a way for high performance simple ITO-free OLEDs.

Introduction

Nowadays, organic semiconductors are widely used as active media in optoelectronic devices, such as organic light-emitting diodes (OLEDs), organic solar cells (OSCs) and organic field-effect transistors (OTFTs). In all of these applications, the charge transport within the organic layers plays a key role^{1,2}. Specially, because of the dependence on the carrier recombination, OLEDs have much strict requirement to transport balance between hole and electron.

However, it's still a challenge to achieve excellent carrier balance, because organic semiconductors typically show highly asymmetric hole and electron transport abilities. In most case, their hole mobility is higher than electron mobility³. As a result, the number of holes in the emitting layer is always larger than that of electrons. However, in the absence of electrons, these excess holes cannot be used to form excitons, and they will also have a destructive effect on the formed excitons due to interactions between hole polarons and excitons⁴.

Charge balance in OLEDs can be improved by either increasing electron mobility or decreasing hole mobility. Till now, many efforts have been made to improve electron mobility, especially by n-doping materials with low electron affinity, such as Cs,

C₆₀, Sn, TIPS-pentacene et al⁵⁻⁷. However, dopants with low electron affinity are always not air-stable, and phase separation may occur in these n-doping systems with the operating time goes. Even so, it still lags far behind hole mobility. Additionally, anode buffer layer, such as copper phthalocyanines, metal oxides and polymer, are always used to alleviate the excess holes⁸⁻¹⁰. However, although they are very efficient to improve luminous efficiency, extra manufacture procedure to introduce buffer layer between anode and hole transport layer is still undesired.

Integrating the hole buffer function into hole transport layer or anode will be a simple and effective way to improve carrier balance and luminous efficiency. Poly(3,4-ethylenedioxythiophene) polystyrene sulfonate (PEDOT:PSS), a mixture of poly(3,4-ethylenedioxythiophene) (PEDOT) and polystyrene sulfonate (PSS), is widely used as hole buffer to balance carriers in OLEDs¹¹. In PEDOT:PSS, the polymer surfactant PSS, which is used to disperse and stabilize PEDOT in solvents, is electrically insulating. By introducing less PSS in synthetic process or removing the excess PSS by high-dielectric solvents¹², such as DMSO and methanol, the film conductivity of PEDOT:PSS can be highly improved to 10³ S·cm⁻¹. Therefore, it is also widely used as conductive transparent

ARTICLE

electrode to replace the traditionally used indium tin oxide (ITO). However, till now, not like the PEDOT:PSS buffer layer, PEDOT:PSS transparent electrode still fail to show superior advantages in balancing carrier and improving luminous efficiency because their OLED device performances are only comparable or even inferior to ITO-based devices¹³⁻¹⁵.

Here, highly conductive and PSS-rich PEDOT:PSS films are successfully fabricated by material-saving fabrication process, using PEDOT:PSS methanol aqueous solution. In the case of reserving PSS, film conductivity of PEDOT:PSS films can also be improved greatly by using PEDOT:PSS solution containing a mass of methanol with high dielectric constant. The conformational change is demonstrated to be more important than the removal of PSS in enhancing film conductivity. The existence of PSS is also proved to play a key role in making PEDOT:PSS film serve two functions simultaneously: transparent electrode and hole buffer layer. ITO-free OLEDs based on these dual functional PEDOT:PSS films possess much better carrier balance and luminous efficiency compared to OLEDs based on ITO and PEDOT:PSS containing less PSS.

Experimental Section

PEDOT:PSS film fabrication: All the PEDOT:PSS solution used in this work is Clevis PH 1000 aqueous solution purchased from Luminescence Technology Corp. PSS-rich PEDOT:PSS films are fabricated by ultrasonic spray coating (USC) process, using PEDOT:PSS methanol aqueous solution in which the ratio between methanol and pristine PEDOT:PSS aqueous solution is 1:1, 1:4, 1:9, 1:14 and 1:19, respectively. The USC process is carried on in the air atmosphere by the UC320 system with D series ultrasonic nozzle (Sianonic Technology Co.). During the USC process, glass substrate is placed on the heating platform about 6 cm under the ultrasonic nozzle, while in order to ensure the rapid evaporation of methanol, the heating temperature of the heating platform is set to 50 °C and the solution injection rate is set to 3 mL/min. For comparison, PEDOT:PSS films with low PSS content are obtained by immersing USC PEDOT:PSS films in methanol for ten minutes. Besides, conventional PEDOT:PSS films are also fabricated by spin coating process, using pristine PEDOT:PSS aqueous solution. And then, these PEDOT:PSS films are annealed at 120 °C for 15 min to remove the solvent, including methanol and water.

Device fabrication: Small molecular organic materials, such as 4,4',4''-tris (carbazol-9-yl)-triphenylamine (TCTA), 1,3,5-Tri[(3-pyridyl)-phen-3-yl]benzene (TmPyPB), Bis(4-phenylthieno[3,2-c]pyridinato-C2,N)(acetylacetonato)iridium(III) [PO-01] and bis (3,5-difluoro-2-(2-pyridyl) phenyl-(2-carboxypyridyl) iridium(III) (Firpic) are purchased from Luminescence Technology Corporation. Green phosphorescent material tris (2-phenylpyridine) iridium (III) [Ir(ppy)₃] is obtained from Xi'an p-OLED. The devices are fabricated on pre-coated PEDOT:PSS and commercially pre-coated indium-tin oxide (ITO) anode on glass substrate. Before using them, the substrates are washed carefully by Decon 90, treated three times in ultrasonic baths of deionized water for 5 min each, baked at 120 °C in an oven and finally treated for 3 min in a plasma cleaner chamber. Hole transport layer, emitting layer, electron transport layer and cathode are evaporated by vacuum thermal evaporating process under high vacuum ($\sim 5 \times 10^{-4}$ Pa) at a rate of 1-2 Å s⁻¹ monitored in situ with a quartz oscillator.

Film and Device characterization: Atomic force microscopy (AFM, Dimension Icon, Bruker Co.) is used to investigate film

morphology of PEDOT:PSS films. The static lateral images after droplets fall on the substrate are measured using a contact angle goniometer (JC2000D contact Angle Meter, Powereach Co. Shanghai, China). XPS spectra of PEDOT:PSS films are obtained by Thermo ESCALAB 250 with Al K α radiation. Raman spectra are measured by modular 3D laser Raman microspectroscopy system Nanofinder FLEX2 from Tokyo Instruments Inc. Luminance-current-voltage characteristics and spectra of unpackaged devices are measured simultaneously using Goniophotometric Measurement System GP series based on spectrometer (MCPD-9800, Otsuka Electronics Co. Osaka, Japan) in air at room temperature. The impedance characteristics of the devices are measured at room temperature using precision LCR meter (TH2829C, Tonghui, Changzhou, China). The transient EL characteristic is collected by HOLITA Fluorescence Spectrum Analyser System (HOLITA Co. Beijing, China).

Results and discussion

3.1 PSS-rich PEDOT:PSS films

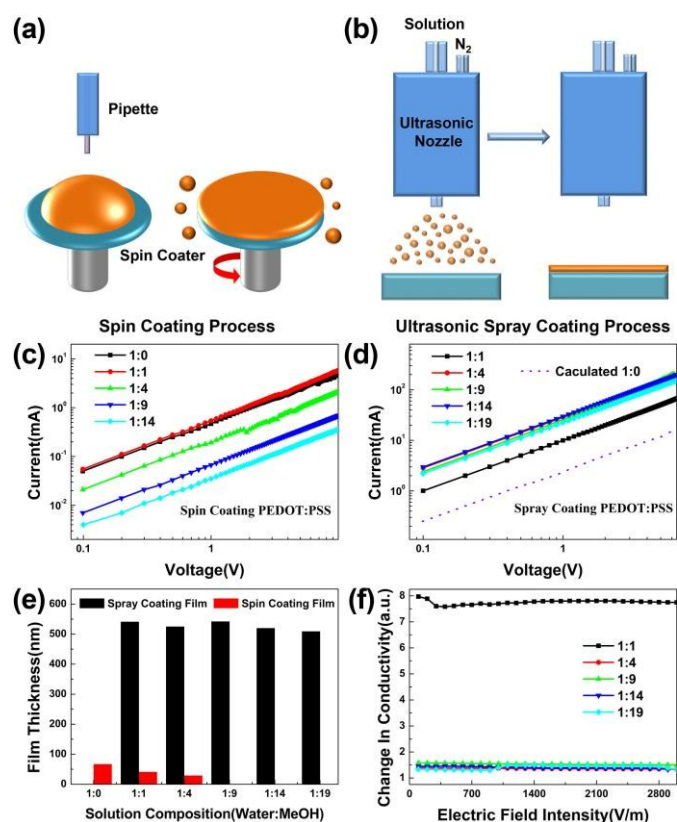


Fig. 1. the schematic diagrams of (a) spin coating process and (b) ultrasonic spray coating (USC) process, the lateral conductivity of (c) spin coating PEDOT:PSS films and (d) USC PEDOT:PSS films, (e) the film thickness of spin coating and USC PEDOT:PSS films and (f) the change of USC PEDOT:PSS films in conductivity after immersing in methanol for ten minutes

Many works demonstrate that film conductivity of PEDOT:PSS can be highly improved by using polar solvent with high dielectric constant as the additive in the aqueous solution or the agent for film posttreatment^{12, 16-18}. According to the reported

papers, the latter method will lead to several orders of magnitude higher conductivity than the former one. It's attributed to that both conformational change and removal of PSS can occur in film posttreatment, while only conformational change can occur in the case of adding additive in the aqueous solution of PEDOT:PSS. However, there is a limitation on the concentration of adding additive, because the concentration of additive over 10% cannot be found in the reported papers using this method. Therefore, the conformational change maybe not sufficient in these PEDOT:PSS films. According to these results, it's hard to identify whether the conformational change or the removal of PSS play a leading role in improving the film conductivity.

To investigate the leading enhancement mechanism, two different fabrication processes are used to prepare PEDOT:PSS films. Ultrasonic spray coating (USC) process is exactly different to spin coating process that is commonly used to fabricate PEDOT:PSS films, as shown in Fig. 1(a) and (b). It has been proved to be a material-saving technology which is suitable to use solution with low solute concentration. Hence, it is chosen to ensure sufficient conformational change without removing PSS in the formation of PEDOT:PSS films, using PEDOT:PSS solution containing a mass of methanol (much more than 10%).

Based on the USC and spin coating process, different types of solution in which the volume ratio between original PEDOT:PSS aqueous solution and methanol additive is 1:0, 1:1, 1:4, 1:9, 1:14 and 1:19, respectively, are used to fabricate PEDOT:PSS films (50, 100, 250, 500, 750 and 1000 μL solution is used, respectively, to ensure the same amount of PEDOT:PSS solute). Their lateral conductivity is studied using the method in Fig. S1, and Fig. 1(c) and (d) show the experimental results. For spin coating process, only PEDOT:PSS film with the ratio of 1:1 (the methanol concentration is 50%) shows slightly enhancement in conductivity compared with the pristine one with the ratio of 1:0. When adding more methanol, the film conductivity of spin coating films decreases obviously with the increase of methanol concentration. It can be explained by the variation of films thickness as shown in Fig. 1(e). Although more solution is used to ensure the same amount of PEDOT:PSS solute, when the concentration of PEDOT:PSS decreases, the thickness of spin coating films decrease. And it even becomes undetectable by profiler when the methanol concentration is over 50%. It's because most solution is removed by centrifugal force and only ultrathin liquid layer absorbed on the substrate is remained in the film formation of spin coating process. That's why highly conductive PEDOT:PSS films have not been demonstrated by using PEDOT:PSS solution containing a mass of methanol (much more than 10%).

Nevertheless, all the PEDOT:PSS solute is used to form film in the USC process with nearly 100% materials utilization. Apparently, the USC films show much higher thicknesses than spin coating films, and their thicknesses nearly remain unchanged with the increase of methanol concentration. It offers the ability to ensure sufficient conformational change without removing PSS in the formation of PEDOT:PSS films. Because the pristine PEDOT:PSS aqueous solution has extremely poor wettability on glass substrate, uniform PEDOT:PSS films cannot be achieved by USC process. The lateral current transport property of PEDOT:PSS film fabricated by spin coating process using the pristine aqueous solution is used to calculate the lateral conductivity of the pristine USC PEDOT:PSS films by considering the influence of

film thickness on conductivity. Apparently, as seen in Fig. 1 (d), the case is exactly different for USC process. Even the PEDOT:PSS film fabricated by solution with the ratio of 1:1 shows more obvious enhancement in conductivity. When the methanol concentration increase from 50% (1:1) to 80% (1:4), an obvious enhancement can also be seen in the conductivity of USC PEDOT:PSS films. And the conductivity change no longer after more methanol is added in PEDOT:PSS solution. It indicates that conformational change is incomplete in the case of adding 50% methanol in the aqueous solution of PEDOT:PSS. But, when the methanol concentration is over 80%, the conformational change becomes a complete state. To weigh the importance of the conformational change and the removal of PSS, these USC films are then treated by immersion in methanol and their conductivity is shown in Fig. 2(f). Only the USC film with incomplete conformational change gets greatly enhanced in conductivity, and no obvious change occurs in the films with complete conformational change. It proves that the conformational change is much more important to improve the film conductivity of PEDOT:PSS than the removal of PSS.

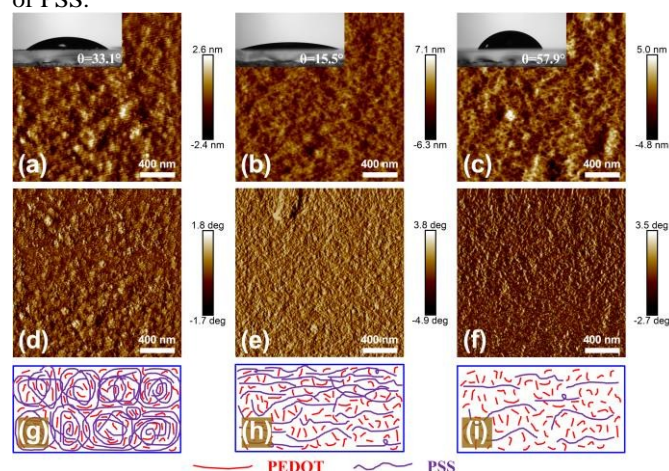


Figure 2. (a)(b)(c) the height images, (d)(e)(f) the phase images and (g)(h)(i) the schematic diagrams of PEDOT:PSS films, including (a) (d) (g) PEDOT-1 films, (b)(e)(h) PEDOT-2 films and (c)(f)(i) PEDOT-3 films, the insets is the contact angle of water on these PEDOT:PSS films.

Evidences from atom force microscope (AFM), X-ray photoelectron spectroscopy (XPS) and Raman spectra also support our speculation about the conformational change and the removal of PSS in these PEDOT:PSS films. Fig. 2 shows the AFM images of these PEDOT:PSS films, including PEDOT-1 fabricated by spin coating process using original aqueous solution, PEDOT-2 fabricated by USC process using aqueous methanol solution (1:14) and PEDOT-3 obtained by immersing PEDOT-2 in methanol for ten minutes. Phase contrast arises from compositional variations of the surface as well as the topographical variations. As seen in Fig. 2, the phase contrast in the PEDOT-1 can be reflected in its topography variation. To make it easier to see, three cross-section curves in the same position of height and phase images are selected and plotted in Fig. S2. Apparently, PEDOT-1 shows similar variation tendency in its height and phase images. However, it's hard to find the connection between phase contrast and topography variation in the PEDOT-2 and PEDOT-3. It indicates that their phase contrast should be mostly caused by compositional variation. Therefore, it gives evidence to support the occurrence of phase separation between PEDOT and PSS chains in PEDOT-2 and PEDOT-3. Besides,

as seen in the phase image of PEDOT-3, one phase seems to be much less than the other. It should be attributed to the removal of PSS by the immersion in methanol. Apparently, PEDOT chains could be released from the entanglement with PSS chains in the film formation under the screening effect of methanol, and a certain amount of PSS chains can be washed off by the immersion in methanol, as shown by the schematic diagrams in Fig. 2(g)-(h). Besides, according to the XPS results shown in Fig. S3, PEDOT-1 and PEDOT-2 have the same PSS content, while there is obvious removal of PSS content in PEDOT-3. The higher contact angle of water on PEDOT-3 also proves the removal of hydrophilic PSS chains. Additionally, the Raman spectra of these three films are also measured and shown in Fig. S4. Compared with PEDOT-1, the band between 1400 and 1500 cm^{-1} , which corresponds to the stretching vibration of $C_{\alpha}=C_{\beta}$ on the five-member ring of PEDOT¹⁹, shifts to red and becomes broad in PEDOT-2 and PEDOT-3. According to the reported results²⁰, it indicates the resonant structure of PEDOT chain in PEDOT-2 and PEDOT-3 changes from a benzoid to a quinoid structure. Considering above, only conformational change occurs in PEDOT-2, and both conformational change and the removal of PSS exist in PEDOT-3. Nevertheless, the similar conductivity makes it clear that the conformational change is more important. Just because of this, highly conductive PSS-rich PEDOT:PSS films with the potential to serve as both transparent electrode and anode buffer layer are firstly achieved here.

3.2 Green OLEDs based on dual-functional PEDOT:PSS films.

As shown in Fig. S5, PEDOT:PSS films can be patterned by the combination of USC process and metal mask. Based on the patterned PSS-rich PEDOT:PSS films, green OLEDs are successfully fabricated and these devices are marked as PE-PSS. The structure and picture of device PE-PSS are shown in Fig.3(a). For comparison, similar devices based on ITO and PEDOT-3 films are also fabricated. The former devices are marked as device ITO, and the latter ones are marked as device PE.

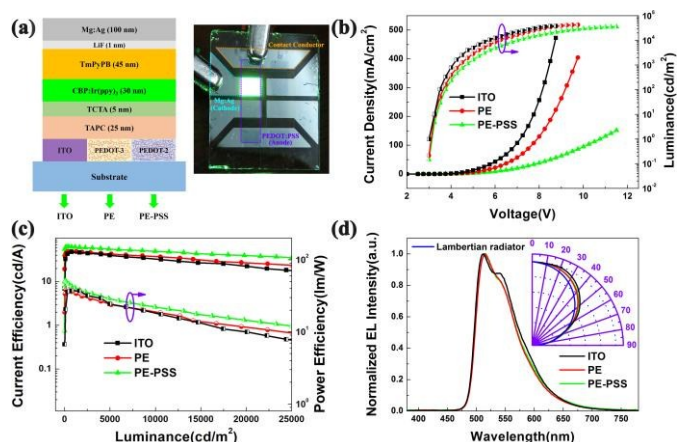


Figure 3. (a) the device structure, (b) the current density-voltage-luminance characteristics, (c) the current efficiency-luminance-power efficiency characteristics and (d) the normalized EL spectra and angular distribution of devices ITO, PE and PE-PSS.

Fig. 3(b) shows the current density-voltage-luminance characteristics of these devices. As seen in Fig. 3(b), the current density of device PE-PSS is much lower than the others, resulting in its low luminance. However, the turn-on voltage of device PE-PSS (3.1 V) is still similar to devices PE (3.1 V) and ITO (3.0 V), indicating the carrier injection in device PE-PSS is still efficient. Furthermore, device PE-PSS performs the best in luminous efficiency among these three devices. The current efficiency-luminance-power efficiency characteristics of these devices are shown in Fig. 3(c). Table 1 summarizes the electroluminescent (EL) performances of devices ITO, PE and PE-PSS. It's clear that device PE is just comparable to device ITO in luminous efficiency. However, device PE-PSS performs much better in maximum current, power and external quantum efficiency compared to the other devices. Besides, device PE-PSS still maintain the advantage in luminous efficiency under high luminance conditions. Under the luminance of 5000 cd/m^2 , the current and external quantum efficiency of device PE-PSS is still more than 30% over those of device ITO. As shown in Fig. 3 (d), device PE-PSS shows no obvious difference with devices PE and ITO in EL spectra and angular distribution. Therefore, to a large extent, the improvement of device PE-PSS in efficiency should be attributed to its better carrier balance.

Device	Turn-on Voltage (V)	Max CE (cd/A)	Max PE (lm/W)	Max EQE (%)	Performances @5000 cd/m^2			
					Voltage(V)	CE(cd/A)	PE(lm/W)	EQE(%)
PE-PSS	3.1	62.4	50.7	17.9	6.1	54.5	28.2	15.7
PE	3.1	48.7	38.0	13.9	5.5	43.4	25.1	12.2
ITO	3.0	47.5	37.3	14.4	5.1	38.2	23.2	11.3

Table 1. the EL performances of devices ITO, PE and PE-PSS.

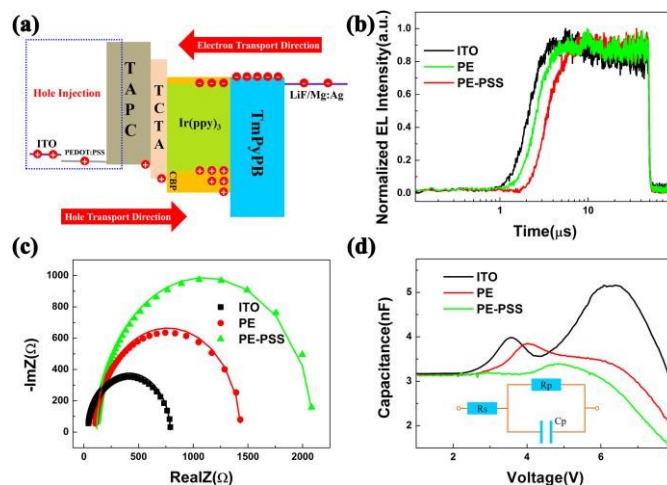


Figure 4. (a) the energy level diagram, (b) the transient EL characteristics, (c) the Cole-Cole plots and (d) the capacitance-voltage characteristics of devices ITO, PE and PE-PSS, the inset is their equivalent circuit model

As shown in Fig. 4 (a), there is only one difference in their transparent anode. Hence, hole injection plays an important role in carrier balance here. To investigate their hole injection behaviors, the transient EL characteristics of these devices are measured and shown in Fig. 4 (b). According to their identical promotion and decay trend, it can be concluded that recombination process isn't affected by their difference.

However, devices ITO, PE and PE-PSS show obvious difference in onset time, as Fig. 4(b) indicates that their onset time is 0.9, 1.1 and 1.6 μs , respectively. It means that the hole injection in device PE-PSS is much slower than the others. Besides, Fig. 4(c) shows the impedance spectroscopy of these three devices. The contact resistance R_s of devices ITO, PE and PE-PSS is 41.5, 105.3 and 118.3 Ω , which is similar to the square resistance of their transparent electrode (38 Ω/\square for ITO, 104 Ω/\square for PEDOT-3, and 128 Ω/\square for PEDOT-2). The higher contact resistance R_s of device PE-PSS should be attributed to the existence of a large number of PSS in PEDOT-2. Nevertheless, device PE-PSS has a much larger bulk resistance R_p than device PE. As a result, the slightly larger R_s has little influence on the performances of device PE-PSS. Additionally, considering the difference between devices PE and PE-PSS, the higher bulk resistance R_p indicates that the existence of a large amount of electrical insulating PSS play a role in alleviating the hole injection in device PE-PSS. In other words, in addition to being transparent electrode, PSS-rich PEDOT-2 film also serves the function of anode buffer layer in device PE-PSS. The extra function is exactly beneficial to improve carrier balance in device.

Charge accumulation at interface will result in the increase of capacitance of multilayer OLED, therefore, the capacitance-voltage characteristics of devices ITO, PE and PE-PSS is measured to analyze their charge balance and the results are shown in Fig. 4(d). When no bias voltage is applied, these three devices has similar capacitance since the capacitance belongs to geometric capacitance. However, different variations occur in their capacitances with the increase of bias voltage. There is obvious increase in the capacitance of devices ITO and PE, indicating that a large number of charges accumulate at the interface in device. Nevertheless, the capacitance of device PE-PSS nearly remains unchanged and just shows tiny change. Conspicuously, carrier balance in device PE-PSS is much better than the others. It's related to the instinct properties of organic semiconductor^{1, 2}. When going from an isolated chain to a system of interacting chains, the lowest unoccupied molecular orbital (LUMO) splitting caused by the interaction of adjacent chains is expected to be much smaller than the highest occupied molecular orbital (HOMO) splitting. As a result, the hole mobility of the organic semiconductors in most cases appear to be higher than the electron mobility by orders of magnitude. That's why the hole blocking effect caused by the large number of electrical insulating PSS is beneficial to improve the carrier balance. The better carrier balance of device PE-PSS can be also directly supported by the current density-voltage characteristics of single carrier devices, as shown in Fig. S6. The results show that device PE-PSS has a comparable hole and electron current density, while the other devices have much larger hole current density.

To investigate the influence of carrier balance on the device performances, the contribution to external quantum efficiency (EQE), polaron and exciton density for devices ITO, PE and PE-PSS are simulated and shown in Fig. 5 and Fig. S7. The results are obtained by solving the exciton dynamics in the phosphorescent system^{21, 22}:

$$\frac{dn_T}{dt} = k_L n_P^2 - k_T n_T - \frac{1}{2} k_{TT} n_T^2 - k_{TP} n_T n_P \quad (1)$$

$$\frac{dn_P}{dt} = \frac{j}{qw} - k_L n_P^2 \quad (2)$$

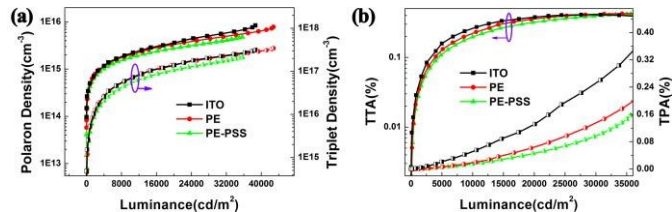


Figure 5. (a) the polaron density, triplet density and (b) the contribution of TTA and TPA to roll-off in Device ITO, PE and PE-PSS

where n_T , n_P , j , q , w , k_{TT} , k_{TP} , k_T is the exciton density, polaron density, current density, elementary charge, width of the recombination zone, triplet-triplet annihilation (TTA) rate constant, triplet-polaron annihilation (TPA) rate constant and Langevin recombination rate constant, respectively. Besides, the fitting parameters used in the simulation are shown in Table S1, and the outcoupling efficiency and EQE at low current density is set to 1. As seen from the simulation result, compared to device PE-PSS, more triplet excitons are needed to achieve the same luminance in devices PE and ITO. It could be attributed to the higher polaron density in devices PE and ITO since the higher polaron density increases the nonradiative transition probabilities of triplet excitons. As a result, as shown in Fig. 5(b), more serious TTA and TPA occur in the devices PE and ITO. Nevertheless, because of the better carrier balance, there is smaller polaron density in device PE-PSS, and a certain luminance can be achieved by lower triplet excitons density. TTA and TPA in device PE-PSS is much weaker under the same luminance, resulting in its higher luminous efficiency. Considering above, the dual-functional PEDOT:PSS films have obvious advantage in improving the carrier balance and luminous efficiency of OLEDs.

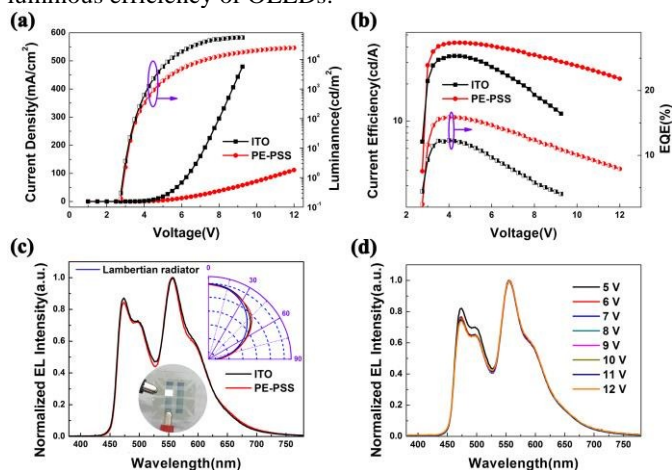


Figure 6. (a) the current density-voltage-luminance characteristics, (b) the current efficiency-voltage-external quantum efficiency characteristics, (c) the normalized EL spectra of white device PE-PSS and ITO-based white device at the luminance of 1000 cd/m^2 and (d) the normalized EL spectra of white device PE-PSS under different bias voltage, the inset is the picture of white device PE-PSS.

3.3 White OLEDs based on dual-functional PEDOT:PSS films.

White OLEDs with the structure shown in Fig. S8 are also fabricated successfully to further verify the superiority of the type of dual-functional PEDOT:PSS films. Besides, ITO-based white OLEDs are also fabricated for comparison. Fig. 6 (a) and (b) shows their current density-voltage-luminance and current efficiency-voltage-EQE characteristics, respectively. The current density of white device PE-PSS is lower than that of ITO-based white device. However, it can be clearly seen that the current efficiency and EQE of white device PE-PSS is much higher than those of ITO-based white device. The maximum power efficiency of white device PE-PSS is 36.3 lm/W, while that of ITO-based white device is only 28.2 lm/W. It indicates that carrier balance in white device can also be obviously improved by using the dual-functional PEDOT:PSS containing of a large number of PSS. Since the PEDOT-2 films also have high transmittance in the visible wavelength range, as shown in Fig. S9, there is no strong microcavity effect in white device PE-PSS. Therefore, as shown in Fig. 6(c), white device PE-PSS doesn't show obvious difference with ITO-based white device in EL spectra and their angular distribution. Additionally, white device PE-PSS also exhibits excellent color stability. Fig. 6(d) shows its normalized EL spectra under different bias voltages. When the bias voltage changes from 5 V to 12 V, the EL spectra nearly keep unchanged. It can also prove that white device PE-PSS remains excellent carrier balance in the whole operating voltage range.

Conclusions

In summary, ultrasonic spray coating process with material-saving property is utilized to fabricate PEDOT:PSS films, using PEDOT:PSS methanol aqueous solution. Due to the screening effect of high concentration methanol, sufficient conformational change occurs in these PEDOT:PSS films so that high conductivity is also achieved, even without removing any PSS chains. When this type of PEDOT:PSS films are used as transparent electrode in OLEDs, they also show obvious buffer effect to hole injection. Based on the dual-functional PEDOT:PSS films, efficient green and white OLEDs with much better carrier balance are successfully achieved. These green devices achieve a maximum current efficiency of 62.4 cd/A, much higher than that of ITO-based OLEDs. And even at the luminance of 5000 cd/m², the current efficiency of these devices can attain to 87% of the maximum. Besides, PEDOT:PSS-based white device achieve the maximum power efficiency of 36.3 lm/W, about 30% higher than that of ITO-based device. This work paves the way to achieve high performance ITO-free OLEDs based on PEDOT:PSS transparent electrode.

Acknowledgements

This work was supported by the National Natural Science Foundation of China (Grant Nos. 61774074, 61475060, 61474054), and Science and Technology Development Planning of Jilin Province (No. 20190101024JH).

Notes and references

State Key Laboratory of Integrated Optoelectronics, College of Electronic Science and Engineering, Jilin University, Changchun, 130012, People's Republic of China

*E-mail: zlt@jlu.edu.cn; xiewf@jlu.edu.cn

- V. Coropceanu, J. Cornil, D. A. da Silva Filho, Y. Olivier, R. Silbey and J.-L. Brédas, *Chem. Rev.*, 2007, 107, 926-952.
- J.-L. Brédas, J. P. Calbert, D. da Silva Filho and J. Cornil, *PNAS*, 2002, 99, 5804-5809.
- L.-S. Cui, S.-B. Ruan, F. Bencheikh, R. Nagata, L. Zhang, K. Inada, H. Nakanotani, L.-S. Liao and C. Adachi, *Nat. Commun.*, 2017, 8, 2250.
- L. S. Cui, Y. L. Deng, D. P. K. Tsang, Z. Q. Jiang, Q. Zhang, L. S. Liao and C. Adachi, *Adv. Mater.*, 2016, 28, 7620-7625.
- X. Lin, B. Wegner, K. M. Lee, M. A. Fusella, F. Zhang, K. Moudgil, B. P. Rand, S. Barlow, S. R. Marder and N. Koch, *Nat. Mater.*, 2017, 16, 1209.
- H. L. Lv, Z.H. Yang, S. J. H. Ong, C. Wei, H.B. Liao, Y.H. Du, G.B. Ji and Z. J. Xu, *Adv. Funct. Mater.* 2019, DOI: 10.1002/adfm.201900163.
- J. T. E. Quinn, J. Zhu, X. Li, J. Wang and Y. Li, *J. Mater. Chem. C*, 2017, 5, 8654-8681.
- J. Xu, Y. Wang, Q. Chen, Y. Lin, H. Shan, V. Roy and Z. Xu, *J. Mater. Chem. C*, 2016, 4, 7377-7382.
- P. J. Jesuraj, H. Hafeez, S. H. Rhee, D. H. Kim, J. C. Lee, W. H. Lee, D. K. Choi, A. Song, K.-B. Chung and M. Song, *Org. Electron.*, 2018, 56, 254-259.
- S. Ying, J. Yao, Y. Chen and D. Ma, *J. Mater. Chem. C*, 2018, 6, 7070.
- Y. H. Kim, C. Wolf, H. Cho, S. H. Jeong and T. W. Lee, *Adv. Mater.*, 2016, 28, 734-741.
- K. Sun, S. Zhang, P. Li, Y. Xia, X. Zhang, D. Du, F. H. Isikgor and J. Ouyang, *J. Mater. Sci-Mater. El.*, 2015, 26, 4438-4462.
- H. Kang, S. Jung, S. Jeong, G. Kim and K. Lee, *Nat. Commun.*, 2015, 6, 6503.
- J. H. Kim, C. W. Joo, J. Lee, Y. K. Seo, J. W. Han, J. Y. Oh, J. S. Kim, S. Yu, J. H. Lee and J. I. Lee, *Macromol. Rapid Comm.*, 2016, 37, 1427-1433.
- Y. K. Seo, C. W. Joo, J. Lee, J. W. Han, N. S. Cho, K. T. Lim, S. Yu, M. H. Kang, C. Yun and B. H. Choi, *Org. Electron.*, 2017, 42, 348-354.
- D. Alemu, H.-Y. Wei, K.-C. Ho and C.-W. Chu, *Energ. Environ. Sci.*, 2012, 5, 9662-9671.
- S. Savagatrup, E. Chan, S. M. Renteria - Garcia, A. D. Printz, A. V. Zaretski, T. F. O'Connor, D. Rodriguez, E. Valle and D. J. Lipomi, *Adv. Funct. Mater.*, 2015, 25, 427-436.
- H. Shi, C. Liu, Q. Jiang and J. Xu, *Adv. Electron. Mater.*, 2015, 1, 1500017.
- J. Ouyang, Q. Xu, C. W. Chu, Y. Yang, G. Li, J. Shinar, *Polymer*, 2004, 45, 8443-8450.
- M. H. Lee, L. X. Chen, N. Li, F. R. Zhu, *J. Mater. Chem. C*, 2017, 5, 10555-10561.
- C. Murawski, K. Leo and M. C. Gather, *Adv. Mater.*, 2013, 25, 6801-6827.
- C. Li, L. Duan, D. Zhang and Y. Qiu, *ACS Appl. Mater. Inter.*, 2015, 7, 15154-15159.

PSS-rich PEDOT:PSS transparent electrode is proposed to greatly enhance carrier balance in OLEDs by its hole buffer effect. [View Article Online](#)
DOI: 10.1039/C9TC00648F

